Supporting Information for

Control of the Rectifying Effect and Direction by Redox Asymmetry in Rh_2-Based Molecular Diodes

Donglei Bu, Yiqing Xiong, Ying Ning Tan, Miao Meng, Chun Y. Liu*
Department of Chemistry, Jinan University, 601 Huang-Pu Avenue West, Guangzhou 510632, China

Experimental Section

Materials and Methods. Pyrazine, tetra acetate dirhodium (Ⅱ), 2-(4-Pyridyl) ethanethiol ethanol, ether and dichloride methane were obtained from commercial sources and used without further purification. Tetrabutyl ammonium hexafluorophosphate (^{n}Bu$_4$NPF$_6$) was recrystallized before use. The tetra acetate dirhodium (Ⅱ) were synthesized according to literature method.[1]

Preparation of Gold Films. Three types of gold films were used in this study. Transparent gold film was used for UV-vis spectroscopy study, gold on quartz was used for electrochemical measurements and ultra-flat gold was used for other characterizations.

Preparation of transparent gold film and gold film on quartz**.**

First, quartz plates (1 × 4.5 cm^2, thickness 0.2 cm) were washed using piranha solution (concentrated sulfuric acid: 30% hydrogen peroxide = 2:1) followed by water and ethanol sequentially and dried in N_2. Second, a 3 – 5 nm thick Ti layer was deposited on the plate by magnetron sputtering. Finally, a 20 nm thick Au layer was deposited on the Ti layer by magnetron sputtering. For electrochemical measurements a 100 nm Au layer was deposited on the Ti layer by magnetron sputtering.

Preparation of ultra-flat gold film.

Freshly cleaved mica sheets (5 × 5 cm^2) were placed onto a stainless steel sample holder in a high vacuum evaporator (Model TRP-450 Sky Technology Development, Shenyang, China). Gold (99.999 %, Alfa Aesar, Ward Hill, MA) was evaporated at 3 Å/s until 150-200 nm thickness was reached at pressure around 7 × 10^{-6} Torr.[2-3] Then, ultraflat gold with large global flatness is prepared on glass according to the method developed by Hegner et al.[4] and Wagner et al.[5] First, microscope cover slips with a diameter of 12 mm were washed using piranha solution followed by water and ethanol sequentially and dried in N_2. Second, these cover slips were glued by Epotek 377 (Epoxy Technology, Billerica, MA) onto the gold thin films. After bring the cover slips contact with the gold thin film, the samples were annealed at 150 °C for 2 hours, allowing the glue to cure. The cover slip was peeled off from the mica

substrate with a gold film glued on it prior to use.

Preparation of Molecular Diodes. SAMs of 2-(4-pyridyl) ethanethiol were first prepared by soaking gold films in 0.01 mM 2-(4-pyridyl) ethanethiol in ethanol for 1hour at room temperature. The fabrication the studied diodes on the SAMs was performed by repeating the flowing cycle. The SAMs were rinsed with ethanol and dried by nitrogen blow and soaked in a 0.2 mM Rh_2 ethanol solution at -15℃ for 1 hour. Then, the sample was dipped in a 0.1 mM pyrazine solution in ether at room temperature for 10 minutes and rinsed with ethanol followed by drying in a nitrogen stream. After the first cycle is done, the soaking time in both Rh_2 and pyrazine can be reduced to two minutes. For the asymmetric structure of the diblock tetramers, the same Rh_2 complex (***C***, ***H***, or ***F***) was used in the first two layers, but for the third and fourth layers, a different Rh_2 complex was chosen.

Physical measurements.

UV-vis spectroscopy

UV-vis spectra were measured with a Shimadzu UV-3600 UV-vis-NIR spectrophotometer.

Electrochemical measurements

Electrochemical measurements were carried out using a CH Instruments model CHI 660D electrochemical analyzer in a 0.1 M $^{n}Bu_4NPF_6$ solution in CH_2Cl_2 with the studied wires on gold as a working electrode, a Pt-plate as a counter electrode, and an Ag/AgCl reference electrode. The differential potential voltammgrams (DPVs) were taken to measure the redox potentials of the donor and acceptor motifs in each diode. The potential increasement and amplitude were set as 0.004 V and 0.05 V, respectively. The pulse width and period were set as 0.2 s and 0.5 s, respectively. The sampling width was set as 0.0167 s.

AFM image and AFM based nanoshaving

AFM topographic images and AFM based nanoshaving were conducted using an Innova AFM (Bruker, SO#47233) under in a glove box (Vigor, SG1200/750TS). AFM images and nanoshaving were taken with a silicon nitride cantilever with spring constant of 40 N/m (RTESP).

Junction formation and current-voltage measurements by CP-AFM

The I-V measurements were conducted according to the method reported in literature.[6] Molecular junctions were formed by bringing a Pt/Ir coated tip (SCM-PIC-V2 probes, Bruker) into contact with a diblock co-oligomer monolayer. These experiments were performed with a Bruker Innova AFM (Bruker, SO#47233) under in a glove box (Vigor SG1200/750TS). Minimal load force (~ 1 nN) to give stable I-V curves was used to make reproducible contact. We examined the current-voltage (I-V)

characteristics of wires over ± 1.0 V. For each diode, about 70 - 200 curves over more than five sample points were measured.

Wire Length Calculations

The wire lengths were estimated from the X-ray single crystal structures of the Rh_2L units that construct the tetramers. An Rh_2L unit 7.4Å.[7]The length of molecule 2-(4-pyridyl) ethanethiol on gold surface is 6.9Å.[8]

DFT Calculations

All calculations were run using the Gaussian 09 programs (revision A.01).The geometry was optimized for the neutral states at a DFT level using the B3LYP function. The LANL2DZ basic set was employed for rhodium, while 6-31G* for other atoms. Post-processing for visualization of the molecular orbitals generated by the DFT calculations was performed using VMD program. Calculated molecular orbitals are demonstrated in Figure S6.

Supplemental Data

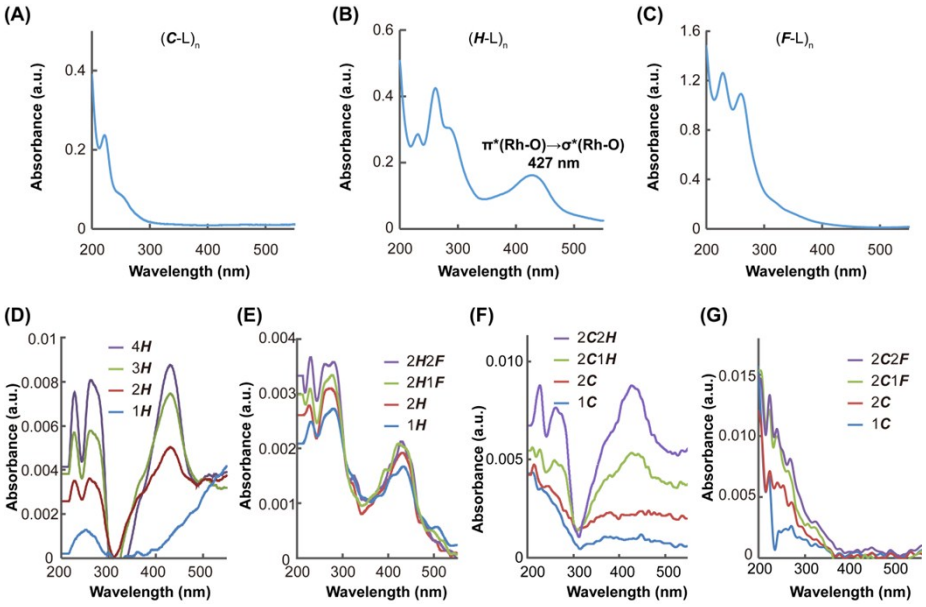

Figure S1. (A-C) UV-vis spectroscopy of (***C***-L)$_n$, (***H***-L)$_n$, (***F***-L)$_n$ oligomers, respectively. (D-F) UV-vis spectroscopy monitoring the fabrication processes of the SAMs, 4***H***, 2***H***2***F***, 2***C***2***H***, and 2***C***2***F***, respectively.

For all these Rh_2 SAMs, the absorption intensity in the UV-Vis spectra increases with increasing the number of the Rh_2 layers, as shown in Fig. S1. For each of them, the spectra are similar, with respect to its layer structures, to those for the corresponding pyrazine-bridged oligomers in solution (see Fig. S1). An absorption band at 426 nm is observed for the $Rh_2(O_2CCH_3)_4$ (***H***) derivatives, which is attributed to a π*(Rh–O)→σ*(Rh–O) transition,[9] but not for the others (Fig S1A-C). Indeed, this

band is absent in the spectra for 2***C***2***H*** having the first and second layer(s) implanted, but present after $Rh_2(O_2CCH_3)_4$ is introduced (Fig S1F). As expected, this transition is observed in the spectra of 4***H***, 2***H***2***F*** and 2***C***2***H***, but not for 2***C***2***F*** (Fig. S1D - G).

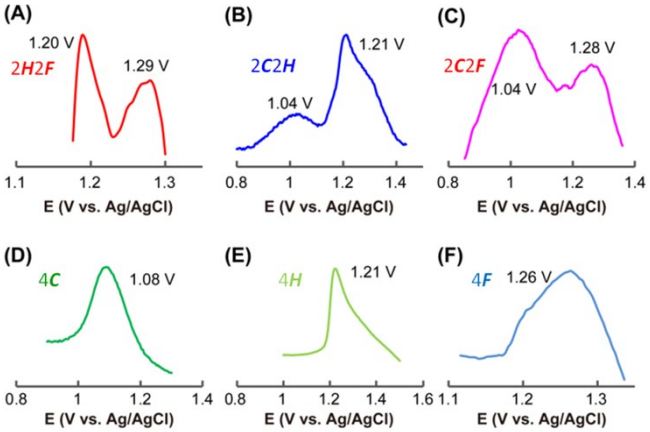

Figure S2. Electrochemical DPVs of (A) 2***H***2***F***, (B) 2***C***2***H***, (C) 2***C***2***F***, (D) 4***C***, (E) 4***H***, and (F) 4***F***, respectively.

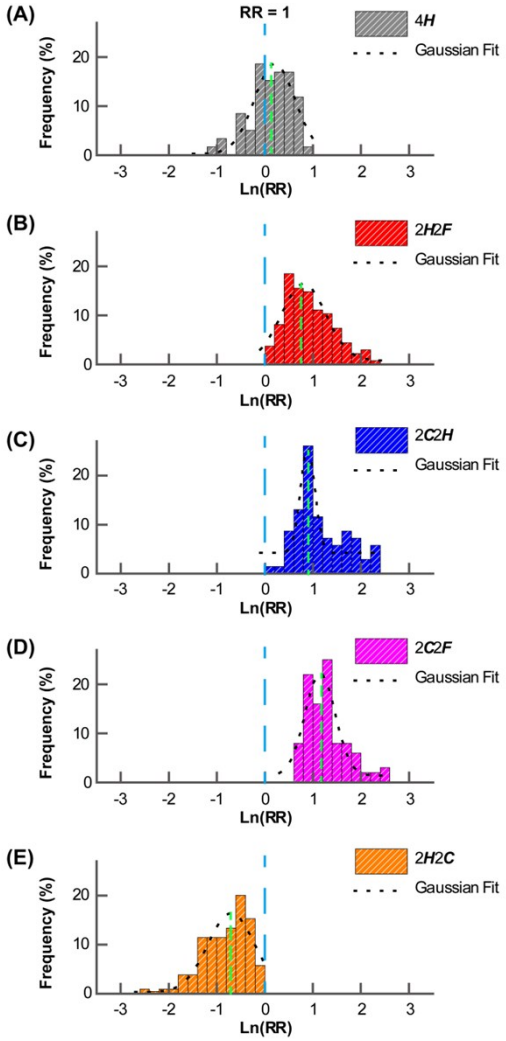

Figure S3. Rectification ratio histograms, presented in Ln(RR) and Gaussian fits for 4***H*** (A), 2***H***2***F*** (B), 2***C***2***H*** (C), 2***C***2***F*** (D), and 2***H***2***C*** (E).

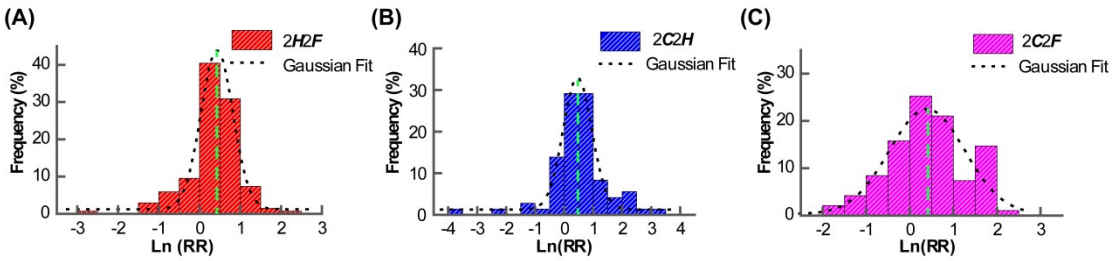

Figure S4. Rectification ratio histogram and Gaussian fit of (A) 2***H***2***F***, (B) 2***C***2***H***, and (C) 2***C***2***F***, respectively, at the lowest bias at which the rectification ratio of diodes reaches 1.5.

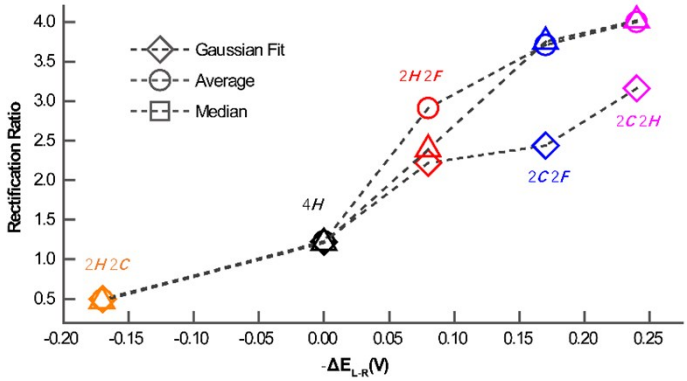

Figure S5. Correlation between the rectification ratio (RR) of studied Rh_2 tetramers and the redox asymmetry ($-\Delta E_{LR}$) for the molecular diode series.

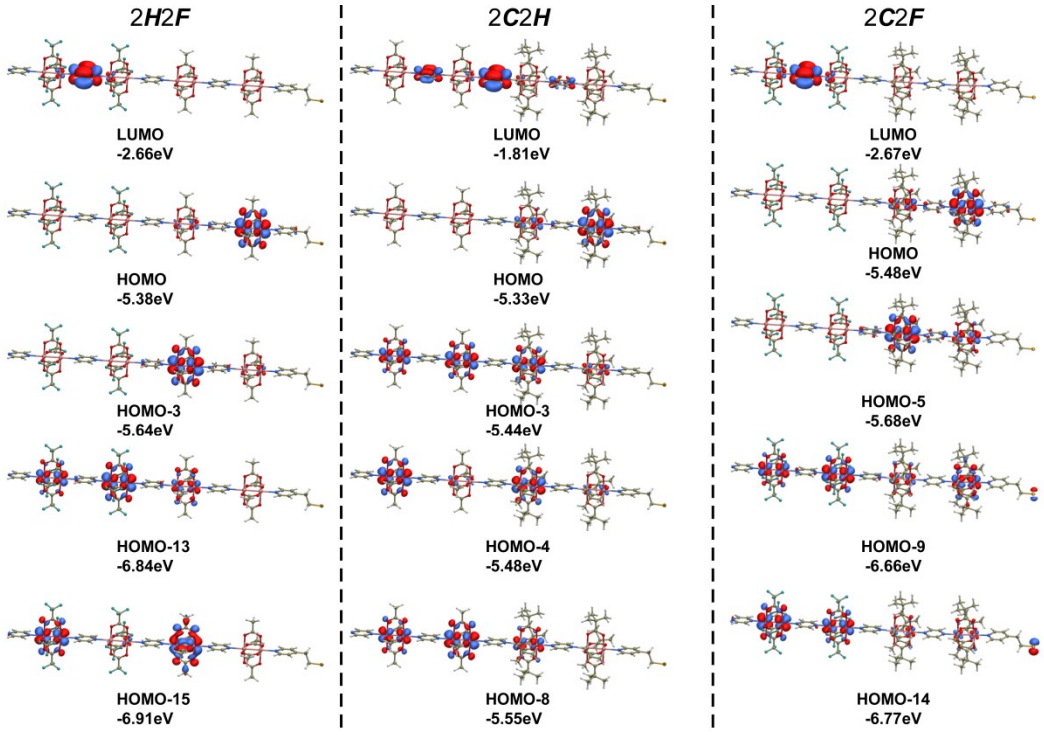

Figure S6. The π(Rh_2)-π(L) conjugated HOMOs and the LUMO generated by DFT calculations for the molecular diodes 2***H***2***F***, (C) 2***C***2***H***, (D) 2***C***2***F***.

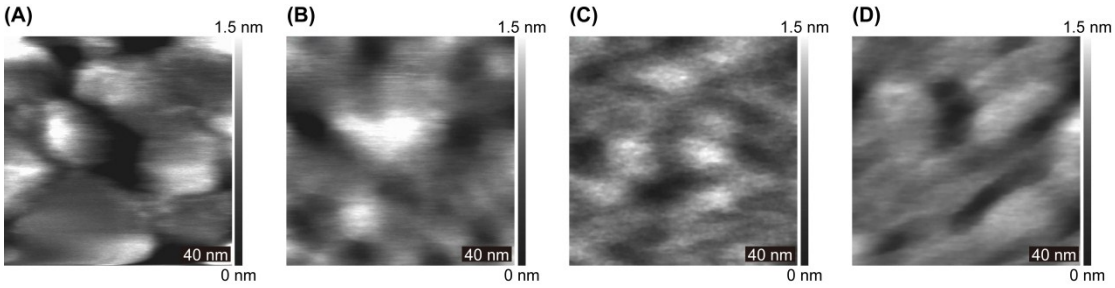

Figure S7. AFM topographic images of (A) bare gold substrate, (B) 2***H***2***F***, (C) 2***C***2***H***, (D) 2***C***2***F*** on gold, respectively. Domains of the assembled molecules (bright regions in (B-D)) as well as defects (dark regions in (B-D)) are observed. The surface roughness of the SAMs is not dramatically increased compared with the gold substrates on which they grew.

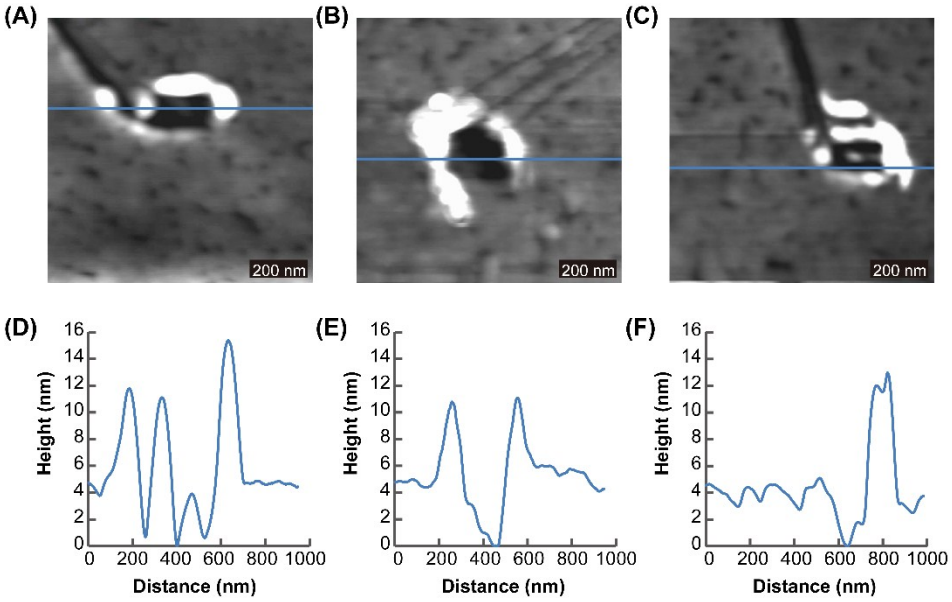

Figure S8. AFM topographic images of (A) 2***H***2***F***, (B) 2***C***2***H***, and (C) 2***C***2***F*** after nano-shaving using an AFM tip, respectively. By removing the implanted molecules on the gold surface, the height differences between the shaved region and surrounding areas were measured, which is considered to be the height of the SAMs. The dark squares in each image are the scratched regions. Molecules removed by the AFM tip aggregate surround the shaved regions and form bright protrusions. From the height difference between the shaved regions and the surrounding SAMs, the thickness of these tetramers is found to be 3-5 nm, which is consistent with the film thickness of ~ 4 nm estimated from the X-ray single crystal structures of the Rh_2L units that construct the tetramers.

[1] Rempel, G. A.; Legzdins, P.; Smith, H.; Wilkinson, G.; Ucko, D. A., Tetrakis(acetato)dirhodium(II) and Similar Carboxylato Compounds. In *Inorganic Syntheses*, John Wiley & Sons, Inc.: **2007**, 90

[2] Bu, D.; Mullen, T. J.; Liu, G.-y.,. *ACS Nano* **2010,** *4* , 6863.

[3] Bu, D.; Riechers, S.; Liang, J.; Liu, G.-y., *Nano Research* **2015,** *8*, 2102.

[4] Hegner, M.; Wagner, P.; Semenza, G., *Surface Science* **1993,** *291*, 39.

[5] Wagner, P.; Hegner, M.; Guentherodt, H.-J.; Semenza, G., *Langmuir* **1995,** *11*, 3867.

[6] Choi, S. H.; Frisbie, C. D., *Journal of the American Chemical Society*, 2010, **132**, 16191.

[7] S. Takamizawa, E.-i. Nakata and T. Saito, *Inorganic Chemistry Communications*, 2003, **6**, 1415.

[8] S. Onaka, M. Yaguchi, R. Yamauchi, T. Ozeki, M. Ito, T. Sunahara, Y. Sugiura, M. Shiotsuka, K. Nunokawa and M. Horibe, *Journal of organometallic chemistry*, 2005, **690**, 57.

[9] F. A. Cotton, E. A. Hillard and C. A. Murillo, *J. Am. Chem. Soc.*, 2002, **124**, 5658.